Dose–response of EBT3 radiochromic films to proton and carbon ion clinical beams

Roberta Castriconi[1], Mario Ciocca[2], Alfredo Mirandola[2], Carla Sini[3], Sara Broggi[3], Marco Schwarz[4,5], Francesco Fracchiolla[4], Mária Martišíková[6,7,8], Giulia Aricò[6,7,8], Giovanni Mettivier[1] and Paolo Russo[1]

[1] Dipartimento di Fisica 'Ettore Pancini', Università di Napoli Federico II, and INFN Sezione di Napoli, Napoli, Italy
[2] Medical Physics Unit, Centro Nazionale di Adroterapia Oncologica, Pavia, Italy
[3] Medical Physics Unit, Ospedale San Raffaele di Milano, Milano, Italy
[4] Medical Physics Unit, Centro di Protonterapia di Trento, Trento, Italy
[5] Trento Institute for Fundamental Physics and Applications (TIFPA), National Institute of Nuclear Physics (INFN), Trento, Italy
[6] Division of Medical Physics in Radiation Oncology, German Cancer Research Center (DKFZ), Heidelberg, Germany
[7] Department of Radiation Oncology and Radiation Therapy, Heidelberg University Hospital, Heidelberg, Germany
[8] Heidelberg Institute for Radiation Oncology (HIRO), Heidelberg, Germany

E-mail: castriconi@na.infn.it

Abstract

We investigated the dose–response of the external beam therapy 3 (EBT3) films for proton and carbon ion clinical beams, in comparison with conventional radiotherapy beams; we also measured the film response along the energy deposition-curve in water. We performed measurements at three hadrontherapy centres by delivering monoenergetic pencil beams (protons: 63–230 MeV; carbon ions: 115–400 MeV/u), at 0.4–20 Gy dose to water, in the plateau of the depth-dose curve. We also irradiated the films to clinical MV-photon and electron beams. We placed the EBT3 films in water along the whole depth-dose curve for 148.8 MeV protons and 398.9 MeV/u carbon ions, in comparison with measurements provided by a plane-parallel ionization chamber. For protons, the response of EBT3 in the plateau of the depth-dose curve is not different from that of photons, within experimental uncertainties. For carbon ions, we observed an energy dependent under-response of EBT3 film, from 16% to 29% with respect to photon beams. Moreover, we observed an under-response in the Bragg peak region of about 10% for 148.8 MeV protons and of about 42% for 398.9 MeV/u carbon ions. For proton and carbon ion clinical beams, an under-response occurs at the Bragg peak. For carbon ions, we also observed an under-response of the EBT3 in the plateau of the depth-dose curve. This effect is the highest at the lowest initial energy of the clinical beams, a phenomenon related to the corresponding higher LET in the film sensitive layer. This behavior should be properly modeled when using EBT3 films for accurate 3D dosimetry.

Keywords: protons, carbon ions, hadrontherapy, radiochromic film dosimetry, EBT3

(Some figures may appear in colour only in the online journal)

1. Introduction

In cancer radiation therapy, an accurate dose determination and a precise dose delivery to the tumour are needed for an optimal treatment in terms of higher tumour control and lower post irradiation complications. Dynamic dose delivery techniques such as intensity modulated photon radiotherapy (IMRT) or active scanning proton and ion beams are increasingly applied in modern radiotherapy. Inhomogeneous fields and steep dose gradients are common in this kind of treatment plans. Therefore, a patient specific quality assurance (QA) pre-treatment verification programme is required to achieve a high spatial and dosimetric accuracy during the treatment delivery. For this purpose, a 3D analysis of dose distribution is required. Since the use of ionization chamber arrays in regions of high dose gradients is limited due to relatively large spacing (mm to cm) and size of individual detector elements (Marinelli *et al* 2015), continuous 2D dosimetric media with high spatial resolution would be preferable (Fuss *et al* 2007). Film dosimetry represents a powerful tool for pre-treatment radiotherapy verification and QA (Todorovic *et al* 2006, Borca *et al* 2013, Sini *et al* 2015). In particular, GAFCHROMIC™ (Ashland Inc.) film models are available that develop a colour change in response to absorption of ionizing radiation: they produce a radiation-induced dose map by the self-developing post-irradiation process (Niroomand-Rad *et al* 1998, Devic 2011).

1.1. Radiochromic dosimetry

GAFCHROMIC™ films (e.g. the latest External Beam Therapy 3 (EBT3) model, introduced in 2012, which replaces previous models for radiotherapy) are radiochromic films adopted routinely for dosimetric verification and QA for conventional radiotherapy. However, their use in hadrontherapy is limited to beam verification and QA procedures (Hara *et al* 2014, Mirandola *et al* 2015). For photon radiotherapy beams, standard procedures for calibration of radiochromic films are routinely adopted (Devic*et al* 2005, 2009, 2016, Martišíková *et al* 2008a, Aldelaijan*et al* 2016). Nevertheless, in case of hadron clinical beams, irradiations with
ions lead to a strongly inhomogeneous dose deposition and a quenching effect affects the film response, at the Bragg peak region (Martišíková *et al* 2008b, Hara *et al* 2014). This effect depends on the linear energy transfer (LET) of the radiation and has significant consequences in the case of protons and carbon ions that lose energy mainly at the end of their path (Bragg peak region) where the LET increases and the dosimeter response decreases (Mašík r ti
ová

et al 2008b, Zhao and Das 2010, Fiorini *et al* 2014, Reinhardt *et al* 2012, Cirrone *et al* 2013, Vadrucci *et al* 2015). The film darkening effect determined by the presence of organic monomers (which polymerize under irradiation and allows measuring an increased optical absorption with increased absorbed dose) is compromised at high-LET irradiations, due to the interplay between density of ionization events along the polymerization sites and their spatial density in the sensitive layer (Kirby *et al* 2010).

1.2. Response of EBT film to protons and carbon ions

Martišíková and Jäkel (2010) investigated the radiochromic EBT film's dose–response and the corresponding quenching effect with proton and carbon ion beams, as a function of the ion type and energy, in the plateau region of the depth-dose curve for monoenergetic beams. To quantify this effect, the relative efficiency, RE, of the EBT film model were used. In accordance to the relative biological effectiveness, the RE was defined as the ratio of doses of photons, D_{photon}, to that of ions, D_{ion}, needed to produce the same film darkening, netΔOD, as the one measured in the films irradiated by ions (Martišíková and Jäkel 2010):

$$\text{RE} = \left.\frac{D_{\text{photon}}}{D_{\text{ion}}}\right|_{\text{net}\Delta\text{OD}}. \tag{1.1}$$

Then, the dose–response relationship for proton and carbon ions of different monoenergetic beams is compared to that of photons (dose–response for ^{60}Co photons in Martišíková *et al* 2008a). Within uncertainties, the curves for protons coincided with the curve for ^{60}Co; all trends for carbon ion showed an under-response of the film over the whole dose range (0.2–20 Gy) in comparison to ^{60}Co beams. Then, for proton beams, the RE was compatible with unity, and there were no significant differences at the various energies. For carbon ions the RE was about 0.7 for all energies—corresponding to a quenching of about 30%—while no dependence on the dose and thus on the fluence was observed (Martišíková and Jäkel 2010).

Zhao and Das (2010) studied the response of the EBT films in order to obtain the depth-dose curve for the depth-dose verification of active scanning proton beams. The film response was strongly dependent on the proton energy at the Bragg peak, where the quenching effect occurs. Their comparison of depth-dose curves measured by EBT films with those measured by an ionization chamber, for several monoenergetic proton beams (76 MeV–186 MeV), showed a good agreement, except for the peak-to-plateau ratio, which was lower for films. The depth-dose curves obtained with the EBT film showed a 10%–20% dose reduction at the Bragg peak (Zhao and Das 2010).

Martišíková *et al* (2008b) and Hara *et al* (2014) investigated the response of the EBT and EBT2 film models, respectively, for the depth-dose verification of active scanning carbon ion beams. The results of the depth-dose distributions measured with the films and an ionization chamber (performed in a water tank) showed that the quenching effect was significant toward the Bragg peak. This was interpreted as a dependence of the response of the sensitive layer of the film on the energy-dependent LET of the particles, whose largest variation occurs at the distal end of the depth-dose curve across the Bragg peak. However, the peak positions are in good agreement with those measured with the ion chamber.

In order to obtain precise results on the spatial distribution of the absorbed dose in tissue exposed to ion beams from dose images achieved with EBT3 radiochromic films, suitable corrections of the acquired data are necessary: two different correction procedures were recently proposed (Fiorini *et al* 2014, Gambarini *et al* 2015).

1.3. This work

Following initial preliminary work (Castriconi *et al* 2016), the aim of this work was to investigate the response of the EBT3 films to proton and carbon ion clinical beams, compared to photon and electron beams response, with the ultimate goal of establishing a proper dose–response correction procedure. This work with the EBT3 film follows the characterization reported by Martišíková and Jäkel (2010) with the old–type EBT film, at one facility. Here, we characterized the new type EBT3 film at three different hadrontherapy centers, in a comparable energy range. Moreover, we presented an analysis of the quenching effect, following a complete characterization of the response of the EBT3 films as a function of the applied dose in monoenergetic photon, electron, proton and carbon ion beams. First, a quantitative comparison was carried out between the EBT3 film response to particle beams (in the plateau region of the depth-dose curve in water) and to conventional radiotherapy beams, at fixed dose values. Then, we performed a measurement of the depth-dose distribution in water and compared the response of the EBT3 films with that obtained using an ionization chamber, to assess the quenching effect along the direction of the beam. The results of this work may contribute to establishing a procedure for film dosimetry in heavy ion beams, characterized in terms of ion type and ion kinetic energy.

2. Materials and methods

2.1. The GAFCHROMIC™ EBT3 film

The GAFCHROMIC™ EBT3 radiochromic film contains a 28 μm thick single active layer (GAFCHROMIC 2016), with a composition different from that of the old–type EBT film (Devic *et al* 2005, 2016). The EBT3 film is nearly tissue equivalent (Gomà *et al* 2013) and it can be immersed in water: its high spatial resolution, energy-independence of response and near tissue-equivalence make it suitable for dose distribution measurements in radiation fields with high dose gradients (Fuss *et al* 2007, Hara *et al* 2014) in a wide dose range (1 cGy–40 Gy). The main absorption band in the optical absorption spectra for the EBT3 model is centered at 633 nm (Devic *et al* 2010).

2.2. Film irradiation

We evaluated the dose–response for GAFCHROMIC™ EBT3 films (lot # 12011401) in the dose range 0.4–20 Gy for all radiation beam qualities.

We performed measurements at 'National Center for Oncological Hadrontherapy' (CNAO, Pavia, Italy) and at 'Heidelberg Ion-Beam Therapy Center' (HIT, Heidelberg, Germany) for proton and carbon ion beams; at 'Proton Therapy Center' (CPT, Trento, Italy) for proton beams; at 'San Raffaele Hospital' (HSR, Milan, Italy) for photon and electron beams. The proton beam energies analysed at CNAO were 62.7, 148.8 and 228.6 MeV (corresponding range in water of 30, 151 and 320 mm, respectively) while the carbon beam energies were 115.2, 257.5 and 398.9 MeV/u (corresponding range in water of 30, 130 and 270 mm, respectively). The beam energies analysed at HIT were 149.9 MeV for protons and 250.1 MeV/u for carbon ions (corresponding range in water of 159 mm and 125 mm, respectively). The energies analysed at CPT were 90.0 MeV and 180.0 MeV for protons (corresponding range in water of 63 mm and 216 mm, respectively).

For the irradiations with photon and electron beams (at HSR) we employed the 'Varian CLINAC 2100' linear accelerator, at 6 MV and 18 MV for photons and at 6 MeV and

12 MeV for electrons; in addition, we irradiated films with a ^{60}Co unit ('Leksell Gamma Knife Perfexion').

As regards the consistency of the absorbed dose to water among the clinical centers, all the facilities involved in this study follow the IAEA TRS-398 Code of Practice (IAEA 2000), for the determination of the absorbed dose to water. The CNAO center adopts a correction factor for ^{12}C absolute dose determination (Mirandola *et al* 2015), which was taken into account when reporting the comparison between carbon ion dose–response curves between CNAO and HIT. The relative total uncertainty for delivered dose values was 1% for photons, 2% for protons and 3% for carbon ions (IAEA 2000).

The 8″ × 10″ EBT3 films were cut in nine pieces, each of 4 × 4 cm^2 size, and exposed to different dose values, in order to obtain nine dose points, for all radiation beam qualities. At the three hadrontherapy centers and for each proton and carbon ion beam, a homogeneous field of 6 × 6 cm^2 size was obtained for irradiating the film pieces using the pencil beam-scanning. We increased the particle fluence for each field, in order to obtain the nine desired dose values. For each irradiation, the film piece was placed at the beam isocentre, perpendicular to the incident beam, behind 19 mm of water-equivalent solid RW3 (Goettingen Water 3) slabs. This depth corresponds to 20 mm in water, assuming a relative water-equivalent length for RW3 of 1.048 (as measured by Mirandola *et al* 2015) for protons and carbon ions of 148.80 MeV and 279.97 MeV/u, respectively). Additional RW3 slabs behind the film stabilized the setup.

Likewise, for photons and electrons, we irradiated each film piece with a collimated field of 6 × 6 cm^2 size, by increasing the accelerator monitor units for obtaining increasing dose values. The film for each irradiation was placed at the isocentre, perpendicular to the incident beam, behind acrylic (PMMA) slabs at a depth of dose maximum (water equivalent depth of 15 mm for 6 MV photons, 35 mm for 18 MV photons, 13 mm for 6 MeV electrons and 27 mm for 12 MeV electrons, calculated from the relative depth of dose maximum equal to 1.17 as reported in Huq *et al* 2001). We placed additional PMMA slabs behind the film to provide full back-scattering conditions.

For ^{60}Co irradiation, the maximum field available was 16 × 16 mm^2, and each film was placed inside a water-equivalent solid phantom at the isocentre, then irradiated with a dose rate of 2.94 Gy min^{-1}.

2.3. Depth-dose measurement

We performed irradiations with proton and carbon ion beams at CNAO. Using the active-scanning technique for both proton and carbon ion beams, we obtained a homogeneous irradiation field of 3 × 3 cm^2 size.

For a quantitative comparison of the EBT3 film response, we performed a measurement of the depth-dose curve—under the same beam delivery conditions—with a parallel plate ionization chamber of 0.02 cm^3 sensitive volume (PTW Advanced Markus Chamber, model 34045, PTW Freiburg, Germany) operated in a 30 × 30 × 30 cm^3 water phantom (PTW model 41023). The phantom contains a holder for the precise positioning of the chamber. The holder position can be varied along the beam (longitudinal) direction using an adjustable spindle drive (0.1 mm step), with a depth range between 20 mm and 264 mm. In order to perform the measurement of the Bragg peak position at 270 mm in water, an extra 4.8 cm thick RW3 slab-phantom (corresponding to 5 cm of water) was added in front of the entrance window of the water phantom.

The EBT3 films were cut in pieces, each of 8 × 4 cm^2 size, and exposed at different positions (along the depth-dose curve of the corresponding ion) in the water tank, perpendicular to the

incident beam. After the irradiation, the EBT3 pieces were analyzed as described in section 2.4; for each film, we converted the net optical densities into dose values using the calibration curve realized respectively for 148.8 MeV protons and 398.9 MeV/u carbon ions. We repeated this procedure for all pieces irradiated at the different position along the depth-dose curve in water. The entrance dose value was set to 1 Gy. The energy investigated for protons was 148.8 MeV and the plateau-to-peak dose value for this energy was 23%. For carbon ions, the energy was 398.9 MeV/u and the plateau-to-peak value for this energy was 33%.

2.4. Film scanning

An Epson Perfection V750 Pro flat-bed scanner was used in transmission mode with 72 dpi scanning resolution. Each film piece was placed (with the same original orientation relative to the film sheet) in the landscape orientation in the middle of the flat-bed scanner (using a template) and then scanned three times consecutively, both before and after irradiation, in order to account for scanner operation fluctuations. Five film pieces provided control films (zero-dose film pieces), in order to quantify the absorbance changes due to environment conditions. The control film represents an unirradiated film piece, which experienced the same history of the irradiated films, except the irradiation (Aldelaijan *et al* 2016). The zero-light transmitted intensity value, which characterizes the background signal of the scanner, was determined with three scans of a black opaque matte cardboard. We analyzed the films only in the red channel of the 48-bit RGB mode, since this channel provided the highest response. We scanned the exposed films as well as the control films 24 h after exposure. Multichannel analysis of radiochromic films (Micke *et al* 2011, Mendez *et al* 2014) was not performed since it is not standard in routine clinical work with radiochromic films.

In order to investigate the variation with the scanning time of the EPSON V750 Pro scanner, we scanned 100 times consecutively (1 h total scan time) an un-irradiated piece and an irradiated (2 Gy) piece of EBT3 film. Data in figure S1 (in supplementary material) (stacks.iop.org/PMB/17/377/mmedia) show that the relative maximum variation in pixel values, $(\max - \min)/(\max + \min)$, was as small as 0.7% (un-irradiated film) and 1.3% (irradiated film): hence, for our three-times repetition of the piece scan, we neglected this effect in the calculation of relative uncertainty of the film response.

In order to average out the film response, for the same piece, the pixel values were sampled over three regions of interest (ROIs) ($1 \times 1\,\mathrm{cm}^2$ size) in the same position as the before-irradiated image and as the after-irradiated image. This operation was repeated for the three scans of each piece. In addition, in order to minimize the impact of the black cardboard non-uniformity, the pixel values were sampled over ten ROIs ($1 \times 1\,\mathrm{cm}^2$ size) in the area corresponding to the middle of the flat-bed scanner. The average level of the background signal was then subtracted from the average level of the unexposed and exposed film pieces (Devic *et al* 2016).

The optical density of the scanned film was defined as:

$$\mathrm{OD} = \log_{10}\left(\frac{\mathrm{PV}_0}{\mathrm{PV}_{\mathrm{film}}}\right) \tag{2.1}$$

where $\mathrm{PV}_{\mathrm{film}}$ is the pixel value in a given position in the film and $\mathrm{PV}_0 = 2^{16}$ is the maximum pixel value.

In order to account for the intrinsic optical density of the film before exposure, one takes the difference of the optical densities of exposed and unexposed films (Devic *et al* 2005); then, by evaluation of the average value in a ROI and subtraction of the background, one obtains the expression for the optical density taking into account all the effects previously mentioned:

$$\Delta\mathrm{OD} = \log_{10}\left(\frac{\overline{\mathrm{PV}}_{\mathrm{unexp}} - \overline{\mathrm{PV}}_{\mathrm{bckg}}}{\overline{\mathrm{PV}}_{\mathrm{exp}} - \overline{\mathrm{PV}}_{\mathrm{bckg}}}\right) \tag{2.2}$$

where $\overline{\mathrm{PV}}$ ($\overline{\mathrm{PV}}_{\mathrm{unexp}}$ for unexposed film, $\overline{\mathrm{PV}}_{\mathrm{exp}}$ for exposed film and $\overline{\mathrm{PV}}_{\mathrm{bckg}}$ for black cardboard, respectively) is the average pixel value determined as a weighted mean of pixel values over the ROIs, where the corresponding weights are the standard deviations of pixel values in each ROI. The uncertainty $\sigma_{\Delta\mathrm{OD}}$ (standard error) of the darkening was determined through error-propagation analysis.

The net optical density change, netΔOD, is used to quantify the darkening of the film:

$$\mathrm{net}\Delta\mathrm{OD} = \Delta\mathrm{OD} - \Delta\mathrm{OD}_{\mathrm{ctrl}} = \log_{10}\left(\frac{\overline{\mathrm{PV}}_{\mathrm{unexp}} - \overline{\mathrm{PV}}_{\mathrm{bckg}}}{\overline{\mathrm{PV}}_{\mathrm{exp}} - \overline{\mathrm{PV}}_{\mathrm{bckg}}}\right) - \log_{10}\left(\frac{\overline{\mathrm{PV}}^{\mathrm{ctrl}}_{\mathrm{unexp}} - \overline{\mathrm{PV}}_{\mathrm{bckg}}}{\overline{\mathrm{PV}}^{\mathrm{ctrl}}_{\mathrm{exp}} - \overline{\mathrm{PV}}_{\mathrm{bckg}}}\right) \tag{2.3}$$

where $\Delta\mathrm{OD}_{\mathrm{ctrl}}$ is the optical density of the control film. The corresponding uncertainty is given by summing in quadrature $\sigma_{\Delta\mathrm{OD}}\sigma_{\Delta\mathrm{OD}_{\mathrm{ctrl}}}$ and the uncertainty on the optical density of the control film.

3. Results

3.1. Dose–response curves

In order to assess the film response for each beam quality, the dose delivered (D), expressed as dose to water, was plotted as a function of the response (netΔOD) of the corresponding film piece. For the calibration curve, two possible fitting functions were investigated for all radiation beam qualities (with a and b fit parameters):

$$D = a \cdot \mathrm{net}\Delta\mathrm{OD} + b \cdot \mathrm{net}\Delta\mathrm{OD}^3 \tag{3.1}$$

$$D = a \cdot \mathrm{net}\Delta\mathrm{OD} \cdot \mathrm{e}^{b\cdot\mathrm{net}\Delta\mathrm{OD}} \tag{3.2}$$

The expression of each function was used to recalculate the dose values and the corresponding error (as a result of the experimental uncertainty and fitting error); then the relative errors were compared. The relative standard error, $\sigma_{\mathrm{D}}(\%)$, expressed in percent, was obtained through the error-propagation of the corresponding fitting function divided by the corresponding recalculated dose value, D_{fit}. In propagating the error, the experimental uncertainty ($\sigma_{\mathrm{net}\Delta\mathrm{OD}}$) and the fitting errors (σ_a and σ_b) were taken into account. For the choice of the best fitting function, the selection criterion was based on the analysis of the $\widetilde{\chi}^2$ and on the total relative error $\sigma_{\mathrm{D}}(\%)$. We determined that the cubic function (3.1) provided lower $\widetilde{\chi}^2$ with respect to the exponential (3.2) function. In terms of total relative errors, the cubic-like function (3.1) provided the best agreement between the goodness-of-fit (in terms reduced chi-square $\widetilde{\chi}^2$) and fit precision (in terms of $\sigma_{\mathrm{D}}(\%)$) when the dose was calculated from the fitting curve (figure 1). This analysis was repeated for all radiation beam qualities. The total relative error was less than 2% for all radiation beam type, beam energies and doses (except that for the 62.7 MeV proton beam, for which the total error was less than 3%).

3.2. Response of EBT3 films to protons and carbon ions relative to photons

Following Martišíková *et al* (2008b) and Martišíková and Jäkel (2010), we calculated the RE (equation (1.1)), using the measured values of the dose–response relationship.

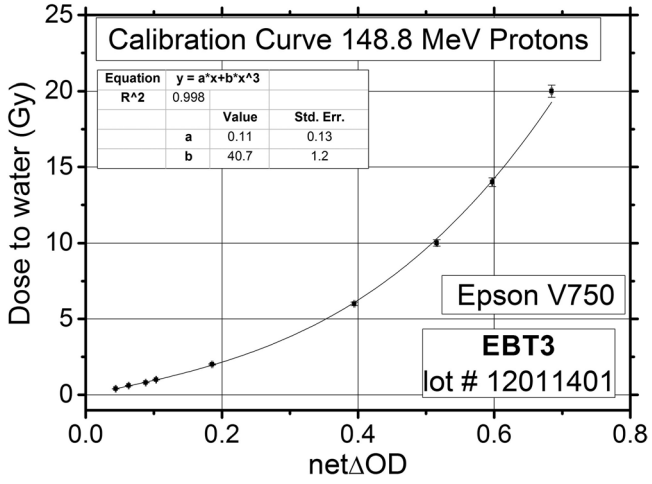

Figure 1. Dose to water as a function of the net optical density change for proton beam of 148.8 MeV with corresponding cubic-like calibration fitting function.

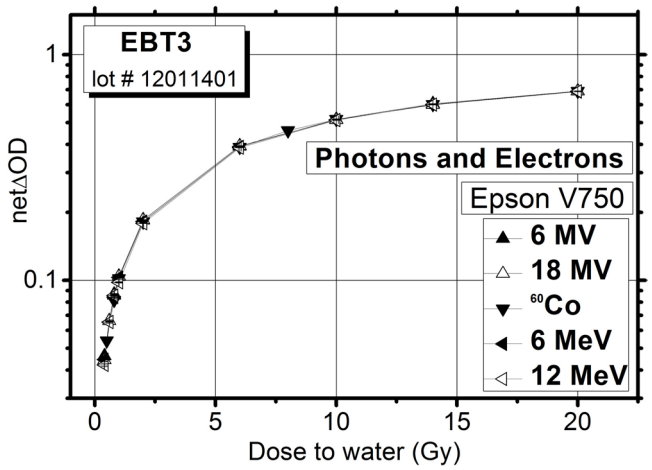

Figure 2. The measured dose–response curves for different energies of photon and electron beams.

Since, for the energies and dose levels investigated, the dose–response for photons was the same as that for electrons (figure 2), we will consider only the comparison between particle beams and 6 MV photon responses. Then, using the netΔOD obtained for the films irradiated by ions, we extracted the dose values for photons from the corresponding calibration fit curve.

Figure 3(a) shows the dose–response for protons and for 6 MV photons, and figure 4(a) shows the corresponding RE data as a function of the photon dose. For all energies, the 1σ uncertainty of the relative-response, σ_{RE}, is in the order of 0.03. As shown in figure 3(a), the curves measured for protons at all energies are practically coincident with that for irradiation with photons. Indeed, the RE for protons in figure 4(a) shows an almost constant trend: a weighted linear fit to all data points pooled together gives a slope consistent with zero and

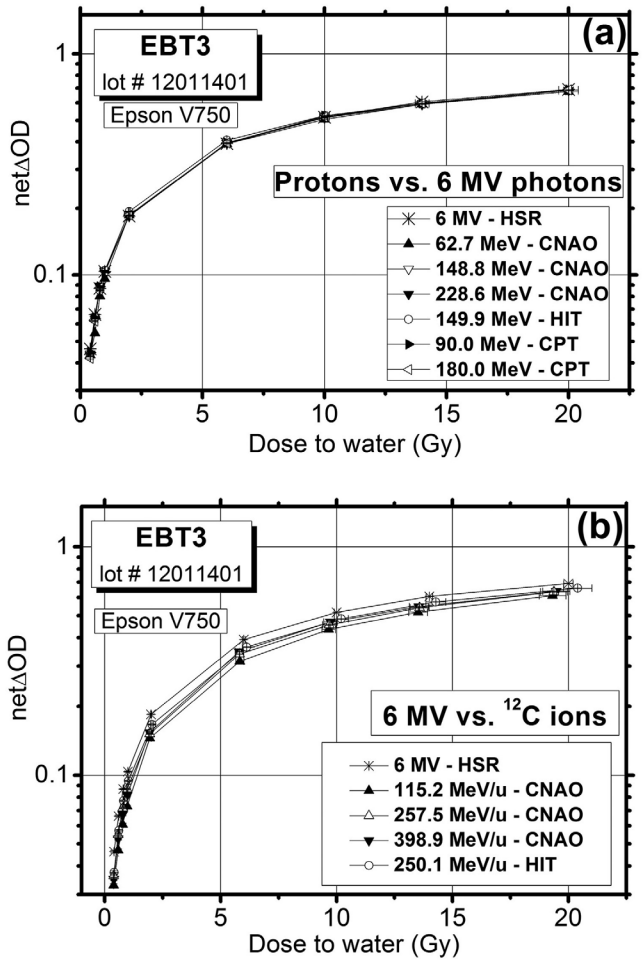

Figure 3. (a) The dose–response relationship for protons and for 6 MV photons; (b) the dose–response for carbon ions in comparison to 6 MV photons.

an intercept of 0.985. Given the 1σ uncertainty of 0.03 on all RE values, then we conclude that the RE value of 0.985 for protons does not differ significantly from unity. Hence, we can conclude that for protons in the ranges 63–230 MeV and 0.4–20 Gy, the response of EBT3 film (in the plateau region of the depth-dose curve) is not different from that of photons, within experimental uncertainties.

Figure 3(b) shows the dose-response data for carbon ions in comparison to 6 MV photons, for the four ion energies investigated in this work. Figure 4(b) shows the corresponding RE curves as a function of the photon dose. For all energies, the 1σ uncertainty of the relative-response is 0.03. The curves in figure 3(b)) show a clear under-response of the EBT3 film over the whole dose range in comparison to 6 MV photon beams.

Indeed, the RE of carbon ions was less than 1 (at 115.2, 250.1, 257.5 and 398.9 MeV/u) and showed a different almost-constant trend for different initial energy of the ions (figure 4(b)). Hence, it was not feasible to evaluate all the data with a unique linear fit, as was done for the RE of protons. By considering the intercept of individual linear fits to each energy dataset

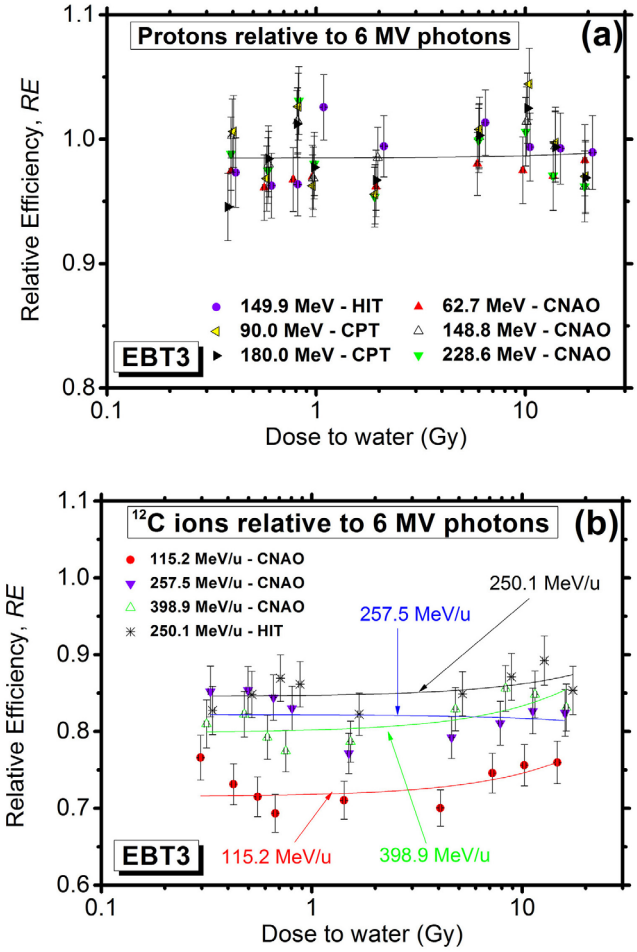

Figure 4. (a) RE data for protons as a function of the photon dose; the graph also shows the linear fitting function when all data points at the different energies are pooled; (b) RE curves for carbon ions as a function of the photon dose; the graph also shows the linear fits (RE versus dose) for the different energies.

(figure 4(b)), it can be seen that for carbon ions, in the range 115–400 MeV/u, the response of the EBT3 film may be dependent on the initial ion energy and a quenching effect occurs. Taking into account the 1σ uncertainty (0.03) on RE values, the measurements indicate that, in the plateau region of the carbon ion depth-dose curve, the RE of the EBT3 film is significantly different from unity.

In particular, the RE derived from individual linear fits (intercept) is 0.71 at 115.2 MeV/u (corresponding to 29% under-response); 0.80 at 398.9 MeV/u (20% under-response); 0.82 at 257.5 MeV/u (18% under-response); and 0.84 at 250.1 MeV/u (16% under-response).

Figure 4(b) shows that the lowest RE (0.71) corresponds to the lowest ion energy (115.2 MeV/u), and the data at 250.1, 257.5 and 398.9 MeV/u have similar RE values (0.84, 0.82 and 0.80, respectively), within a 1σ uncertainty of 0.03. In particular, the RE measured at HIT at 250.1 MeV/u (0.84) is consistent with the one measured at CNAO at 257.5 MeV/u (0.82).

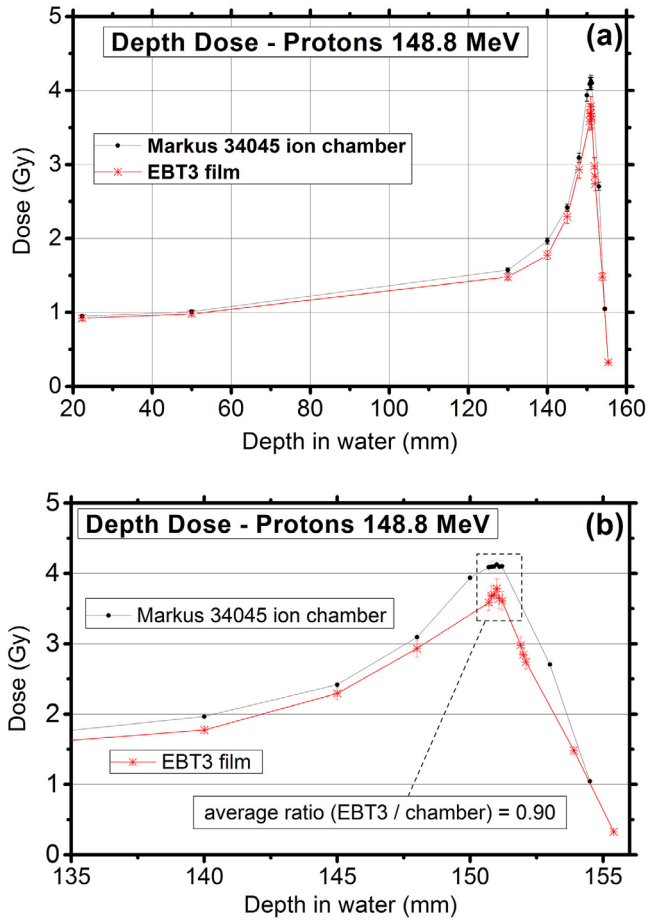

Figure 5. (a) The depth-dose curves obtained for protons, with EBT3 film and Markus chamber; (b) the same data are shown only in the region of the Bragg peak, where quenching occurs for the EBT3 film response.

3.3. Depth-dose curve in water for protons and carbon ions

Figure 5(a) shows the depth-dose curves obtained for protons, with the EBT3 film and with the Markus chamber, with data replotted in figure 5(b) only in the Bragg peak region, where the EBT3 film curve presented a slight under-response. The average ratio of the dose values measured with EBT3 and Markus chamber in the Bragg peak region (150.8–151.2 mm depth) was 0.90 $\pm$ 0.04, corresponding to an under-response of about 10%.

Figure 6(a) shows the depth-dose curves obtained for carbon ions, with the EBT3 films and with the Markus chamber. Figure 6(b) shows the same comparison only in the Bragg peak region, where quenching clearly occurs for the EBT3 film response. The average ratio of the dose values measured with EBT3 and Markus chamber in the Bragg peak region (269.2–269.6 mm depth) was 0.58 $\pm$ 0.02 corresponding to an under-response of about 42%.

4. Discussion

The total relative error of 2% (0.4–20 Gy) is in overall agreement with current achieved values for the total uncertainty in EBT3 dosimetry with photon beams (Devic *et al* 2016), where uncertainties below ≅2% can be obtained above ≅1 Gy, with a calibration curve in the form $D = a \cdot \text{net}\Delta\text{OD} + b \cdot \text{net}\Delta\text{OD}^n$ with n in the range 2–3 (while $n = 3$ was used in this work). In similar overall agreement for EBT3 films, Sorriaux *et al* (2013) reported a total uncertainty of 1.5% for photons and 60 MeV proton beams in the range 0.4–10 Gy.

4.1. Protons (63–230 MeV)

In the explored energy range, the EBT3 film showed the same response for clinical proton beams—in the plateau region of the depth-dose curve—as for radiotherapy photon beams, independent of the incident proton energy. Therefore, the calibration curve obtained for one proton energy can be used for different proton energies in this range (for a given film batch). This is in agreement with reports (Martišíková and Jäkel 2010) which investigated the response of EBT type radiochromic films. In that paper, the RE for protons was in the range 0.88–1.00 with a 1σ uncertainty of about 0.05 (50–200 MeV); in this work, the average RE was 0.985 (0.4–20 Gy), with a 1σ uncertainty of 0.03 on all RE values. However, we observed an under-response of the EBT3 film at the distal end of the depth-dose curve. For protons of 148.8 MeV initial energy, in the Bragg peak region (150.8–151.2 mm depth), we found that the average ratio of the dose values measured with EBT3 to the dose of the Markus ionization chamber was 0.90 ± 0.04, corresponding to an under-response of about 10%. For the 148.8 MeV protons, the LET at the Bragg peak is ≅3 keV μm^{-1} (see figure 6 in Mirandola *et al* 2015).

An under-response of 10% is in agreement with a recent scientific report (Zhao and Das 2010), which found a value from 10% to 20% for proton energies in the range of 76–186 MeV, for EBT films. A recent result of Vadrucci *et al* (2015) showed an under response up to about 33% for 5 MeV protons (LET = 13 keV μm^{-1}) with respect to ^{60}Co gamma radiation, which is consistent with the LET dependence, already observed with higher energy protons.

4.2. Carbon ions (115–400 MeV/u)

In this work we observed an under-response—in the plateau region of the depth-dose curve—for carbon ion clinical beams. This confirms qualitatively the observations of Martišíková and Jäkel (2010), who used the EBT type film. Given the different total thickness of the sensitive layer and elemental composition of EBT and EBT3 films (Devic *et al* 2005, 2016), a slightly different energy deposition might occur in the two film models, for given ion type and energy. In the present findings, the RE of the EBT3 film is dependent on the incident energy for carbon ions, in the range 115–400 MeV/u, with values in the range 0.67–0.89 (min–max value of all data points). On the other hand, Martišíková and Jäkel (2010) found that for carbon ions, the RE was about 0.7 at all energies (100–400 MeV/u), independent of the dose, with values of RE in the min–max range 0.65–0.78. A graphical comparison of data is presented in figure 7.

For our data at 115.2 MeV/u, the RE was as low as 0.71 and close to the average value observed by Martišíková and Jäkel (2010). On the other hand, for the other energies RE is higher: the corresponding values did not differ within the 1σ uncertainty but are outside the range of values found in Martišíková and Jäkel (2010).

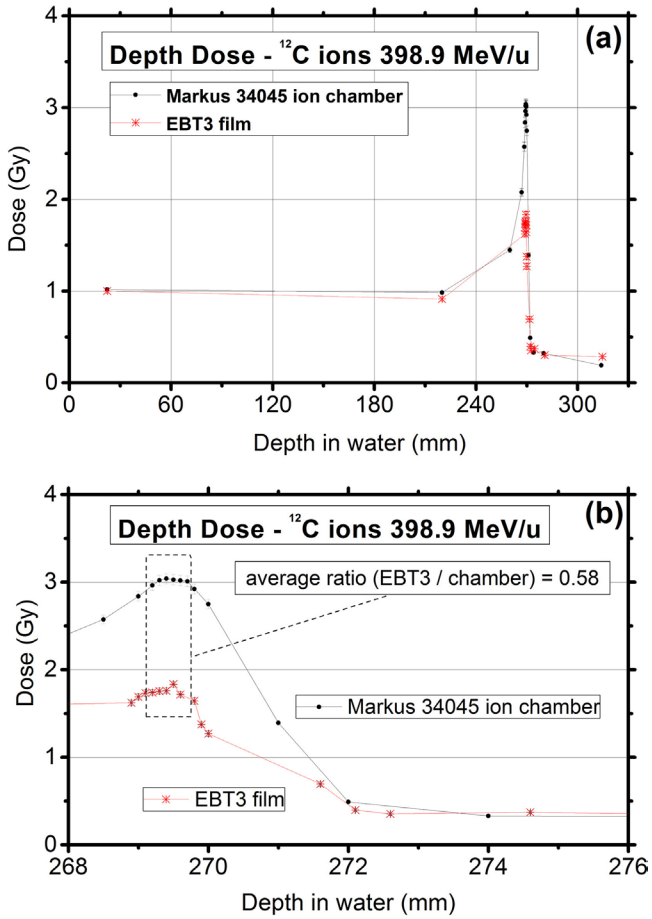

Figure 6. (a) The depth-dose curves for ^{12}C ions obtained with EBT3 film and Markus chamber; (b) the same data are replotted only in the region of the Bragg peak, where quenching occurs for the EBT3 film response.

We relate this behavior to the LET-dependence of the EBT3 response. Indeed, at a depth of 20 mm in water, the LET for 115.2 MeV/u carbon ions ($\cong$40 keV μm^{-1}) is four times greater than that at 257.5 MeV/u or at 398.9 MeV/u ($\cong$10 keV μm^{-1} in both cases) (Mirandola *et al* 2015). If the EBT3 response is LET-dependent, then the RE at the lower energy should be significantly less than at those high energies, in agreement with the above findings. We also note that, while measurements in the present work were made at 20 mm in water, Martišíková and Jäkel (2010) performed measurements at 1.03 mm in water. Since the LET at 1.03 mm in water is not significantly different for carbon ion energies in the range 100–400 MeV/u, their data may be consistent with a negligible dependence on ion energy.

We observed an under-response of the EBT3 film in the Bragg peak region; this is in agreement with data in Martišíková *et al* (2008b) and Hara *et al* (2014).

For carbon ion beams at 398.9 MeV/u, in the Bragg peak (269.2–269.6 mm in water), the average ratio of the dose values measured with EBT3, to those measured with the Markus chamber, was 0.58 $\pm$ 0.02, corresponding to an under-response of 42%. The LET at the Bragg peak is $\cong$30 keV μm^{-1} at 400 MeV/u (Mirandola *et al* 2015).

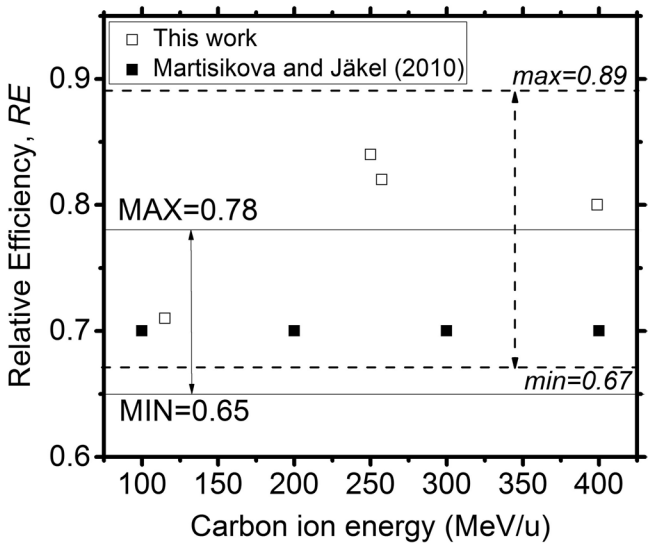

Figure 7. Comparison of RE data (average value and range) for carbon ions in this work and in Martišíková and Jäkel (2010), versus ion energy. The (MAX, MIN) data refer to the range observed in the 2010 paper, while (min, max) are the ranges observed in this work.

The behavior shown above should be properly modeled when using EBT3 films for accurate 3D dosimetry in proton and carbon ion therapy. It is reasonable to assume that the film response to particle irradiation increases as the LET along the depth-dose curve increases, until a threshold value of LET is reached, for which the response is saturated. For protons, this threshold should be in the range 1–3 keV μm^{-1}, approximately, as deduced from our findings. For carbon ions, for which the LET in the plateau is approximately 10 keV μm^{-1}, the film saturation (with respect to photon response) occurs along the whole depth-dose curve. However, in addition to a LET-dependence, there should be also an interaction-specific response of the film, since the under-response observed at 115.2 MeV/u in the plateau region (29%) is lower than at 398.9 MeV/u in the Bragg peak (42%) (LET close to 40 and to 30 keV μm^{-1}, respectively, see Mirandola *et al* 2015).

4.3. Film response simulation and outline of a correction procedure

The rationale of a new correction procedure for EBT3 film under-response may be set forth here, for the specific case of an homogeneous object. Indeed, using Monte Carlo (MC) simulations validated using calibrated ionization chamber dosimeters, it could be possible to recover an accurate dose estimate at any given point in a homogeneous (e.g. water, RW3, PMMA) phantom. This would provide a correction value against the biased dose value measured (for a given ion type and incident kinetic energy) with the EBT3 film, at the measurement point in the phantom. The data for MC validation may come from a limited set of depth-dose profiles measured in the homogeneous sample for a representative set of ion energies. For comparison, in their correction procedure for EBT3 films exposed to clinical proton beams, Gambarini *et al* (2015) used dose values calculated with the clinical treatment planning system coupled to data from a limited number of Bragg peaks. The proposed procedure aims at recovering accurately a dose value corrected for energy-dependent film under-response by using a pre-determined

3D dataset of correction factors adapted for each particular beam energy, E, and ion type, i. The same procedure using pre-calculated correction factors might be adopted in the case of measurements in a non-homogeneous (e.g. lung, brain, torso) phantom, by including the description of the phantom into the MC code.

In the simulations, a pencil beam of monoenergetic particles is incident normally and centrally on the entrance surface of a suitably large sample volume. For a given ion energy and type, dose determinations via MC simulations are made on a 3D mesh of data points inside the water volume. The set of dose determinations for that pencil beam will then give the 'dose point spread function', $\mathrm{dPSF}_{i,E}(x,y,z)$ for that ion type and energy. Then, the dPSF is normalized to unit dose at isocenter. Once the normalized dPSF is determined for a given ion energy, the same simulations can be repeated for all energies of interest, as needed e.g. for spread out Bragg peak scans. We assume the space variant property for dPSF and linear superposition of dose distributions produced by a treatment scan with pencil beams of different energies and different intensities. Then, for a pencil beam scan of a given entrance area in a treatment scan, the convolution of the pre-determined dPSFs could be calculated for determining the actual 3D dose map in the irradiated volume. This map provides a set of 'true' dose values, against which one can correct the dose values determined by the film response using calibration curves measured at the plateau of the energy deposition curve. For protons, the dPSF is almost energy independent, while for carbon ions the dPSF has to be determined for each incident energy of interest.

We planned MC simulation work for evaluating the energy deposition of proton and carbon ion clinical beams in the sensitive layer of the EBT3 film model immersed at different depths in water, so to relate quantitatively the observed quenching effect to the LET of the specific particle radiation, and to the dose deposition by production of secondary particles. A starting point for this investigation is represented by the work of Reinhardt *et al* (2015), who used FLUKA simulations, restricted to proton beams in the 4–20 MeV range. Report and discussion of this simulation work will be the subject of a future paper.

5. Conclusions

We compared the EBT3 film response to particle beams to that of conventional radiotherapy beams, via measurements at three hadrontherapy centers. We observed that the RE of EBT3 film for proton beams was dose independent and energy independent and equal to unity, in the range 63–230 MeV, in agreement with Martišíková and Jäkel (2010).

In the plateau region of the depth-dose curve, we observed a dose independent but energy dependent under-response (from 16% to 29%) of EBT3 film for carbon ions (115–400 MeV/u), with respect to photons. This effect was the highest at the lowest initial energy of the clinical beams, a phenomenon attributed to the corresponding higher LET of carbon ions in the sensitive layer of the film. For comparison, Martišíková and Jäkel (2010) indicated an average under-response of 30% independent of dose and of ion energy, for the EBT film.

In the region of the Bragg peak, we observed an under-response of 10% for 148.8 MeV protons, and an under-response of 42% for 398.9 MeV/u carbon ions. When considering the particle LET at the Bragg peak, we attributed the lower under-response of protons, with respect to carbon ions, to the corresponding lower specific energy loss (3 against 30 keV $\mu\mathrm{m}^{-1}$).

We note that the inclusion of a set of correction factors for film dosimetry with heavy ion beams, with their uncertainties, introduces an additional source of statistical fluctuation and measurement bias. In the case of proton spread out Bragg peaks there is preliminary evidence that energy dependent dose correction factors may deviate between 2% and 8% from

measurements (Fiorini *et al* 2014). For taking into account the variation in film sensitivity due to variation in the thickness of the sensitive layer, Reinhardt *et al* (2015) consider a 5% added uncertainty. However, for carbon ion beams there is still need for additional data. In this regard, the present study may contribute by providing experimental data, to establishing a procedure for film dosimetry in heavy ion beams, for both ion types and a range of kinetic energy.

Acknowledgments

Thanks to the following persons for the access provided to the experimental facilities: Dr S Rossi (CNAO, Pavia, Italy); Dr O Jäkel (HIT, Heidelberg, Germany); Dr R Calandrino, Dr C Fiorino (San Raffaele Hospital, Milan, Italy); Dr M Amichetti (CPT, Trento, Italy). We thank Dr Slobodan Devic (McGill University, Montreal, Canada) for reading the manuscript and valuable comments. This works was carried out in the framework of the project RDH supported by INFN, Italy. MM and GA thank for the funding by the German Cancer Aid (Deutsche Krebshilfe). The authors thank the HIT facility for the beamtime provided for this experiment. Preliminary data of this work were presented as a poster at the 9th National Congress of the Associazione Italiana di Fisica Medica (AIFM), Perugia, Italy, 25–28 February, 2016.

References

Aldelaijan S *et al* 2016 Use of a control film piece in radiochromic film dosimetry *Phys. Medica* **32** 202–7

Borca V C *et al* 2013 Dosimetric characterization and use of GAFCHROMIC EBT3 film for IMRT dose verification *J. Appl. Clin. Med. Phys.* **14** 158–71

Castriconi R *et al* 2016 Characterization of the energy dependent response of EBT3 radiochromic film to proton and carbon ion beams *Phys. Medica* **32** 10–1

Cirrone G A P *et al* 2013 Absolute and relative dosimetry for ELIMED *AIP Conf. Proc.* **1546** 70–80

Devic S 2011 Radiochromic film dosimetry: past, present and future *Phys. Medica* **27** 122–34

Devic S *et al* 2005 Precise radiochromic film dosimetry using a flat-bed document scanner *Med. Phys.* **32** 2245–53

Devic S *et al* 2010 Absorption spectra time evolution of EBT-2 model GAFCHROMIC™ film *Med. Phys.* **37** 2207–14

Devic S, Tomic N and Lewis D 2016 Reference radiochromic film dosimetry: review of technical aspects *Phys. Medica* **32** 541–56

Devic S, Tomic N, Soares C G and Podgorsak E B 2009 Optimizing the dynamic range extension of a radiochromic film dosimetry system *Med. Phys.* **36** 429–37

Fiorini F *et al* 2014 Under-response correction for EBT3 films in the presence of proton spread out Bragg peaks *Phys. Medica* **30** 454–61

Fuss M, Sturtewagen E, De Wagter C and Georg D 2007 Dosimetric characterization of Gafchromic EBT film and its implication on film dosimetry quality assurance *Phys. Med. Biol.* **52** 4211–25

GAFCHROMIC 2016 website: http://www.gafchromic.com/gafchromic-film/radiotherapy-films/EBT/index.asp

Gambarini G *et al* 2015 Study on corrections of dose images obtained with Gafchromic EBT3 films for measurements on phantom irradiated with proton beams *Communicated at ANIMMA 2015, Advancements in Nuclear Instrumentation Measurement Methods and their Applications (Lisbon, Portugal, 20–24 April 2015)*

Gomà C, Andreo P and Sempau J 2013 Spencer–Attix water/medium stopping-power ratios for the dosimetry of proton pencil beams *Phys. Med. Biol.* **58** 2509–22

Hara Y *et al* 2014 Application of radiochromic film for quality assurance in the heavy-ion beam scanning irradiation system at HIMAC *Nucl. Instrum. Methods* B **331** 253–6

Huq M S, Yue N and Suntharalingam N 2001 Experimental determination of depth-scaling factors and central axis depth dose for clinical electron beams *Int. J. Cancer* **96** 232–7
Kirby D *et al* 2010 LET dependence of GafChromic films and an ion chamber in low-energy proton dosimetry *Phys. Med. Biol.* **55** 417–33
IAEA 2000 Absorbed dose determination in external beam radiotherapy: an international code of practice for dosimetry based on standards of absorbed dose to water *Technical Report* Series-398, International Atomic Energy Agency (www-pub.iaea.org/mtcd/publications/pdf/trs398_scr.pdf)
Marinelli M *et al* 2015 Dosimetric characterization of a microDiamond detector in clinical scanned carbon ion beams *Med. Phys.* **42** 2085–93
Martišíková M, Ackermann B and Jäkel O 2008a Analysis of uncertainties in Gafchromic EBT film dosimetry of photon beams *Phys. Med. Biol.* **53** 7013–27
Martišíková M, Ackermann B, Klemm S and Jäkel O 2008b Use of Gafchromic EBT films in heavy ion therapy *Nucl. Instrum. Methods* A **591** 171–2
Martišíková M and Jäkel O 2010 Dosimetric properties of Gafchromic EBT films in monoenergetic medical ion beams *Phys. Med. Biol.* **55** 3741–51
Mendez I *et al* 2014 On multichannel film dosimetry with channel-independent perturbations *Med. Phys.* **41** 011705
Micke A, Lewis D F and Yu X 2011 Multichannel film dosimetry with nonuniformity correction *Med. Phys.* **38** 2523–34
Mirandola A *et al* 2015 Dosimetric commissioning and quality assurance of scanned ion beams at the Italian National Center for Oncological Hadrontherapy *Med. Phys.* **42** 5287–300
Niroomand-Rad A *et al* 1998 Radiochromic film dosimetry: recommendations of AAPM Radiation Therapy Committee Task Group 55 *Med. Phys.* **25** 2093–114
Reinhardt S, Hillbrand M, Wilkens J J and Assmann W 2012 Comparison of Gafchromic EBT2 and EBT3 films for clinical photon and proton beams *Med. Phys.* **39** 5257–62
Reinhardt S *et al* 2015 Investigation of EBT2 and EBT3 films for proton dosimetry in the 4–20 MeV energy range *Radiat. Environ. Biophys.* **54** 71–9
Sini C, Broggi S, Fiorino C, Cattaneo G M, and Calandrino R 2015 Accuracy of dose calculation algorithms for static and rotational IMRT of lung cancer: a phantom study *Phys. Medica* **31** 382–90
Sorriaux J *et al* 2013 Evaluation of Gafchromic EBT3 films characteristics in therapy photon, electron and proton beams *Phys. Medica* **29** 599–606
Todorovic M, Fischer M, Cremers F, Thom E and Schmidt R 2006 Evaluation of GafChromic EBT prototype B for external beam dose verification *Med. Phys.* **33** 1321–8
Vadrucci M *et al* 2015 Calibration of GafChromic EBT3 for absorbed dose measurements in 5 MeV proton beam and ^{60}Co γ-rays *Med. Phys.* **42** 4678–84
Zhao L and Das I J 2010 Gafchromic EBT film dosimetry in proton beams *Phys. Med. Biol.* **55** N291–301